Research in Astron. Astrophys. **2012** Vol. **12** No. **4**, 443–452
http://www.raa-journal.org *http://www.iop.org/journals/raa*

***R**esearch in*
***A**stronomy and*
***A**strophysics*

M dwarf stars — the by-product of X-ray selected AGN candidates *

Yu Bai[1], Yan-Chun Sun[1], Xiang-Tao He[1], Yang Chen[1], Jiang-Hua Wu[1], Qing-Kang Li[1], Richard F. Green[2] and Wolfgang Voges[3]

[1] Department of Astronomy, Beijing Normal University, Beijing 100875, China; *baiyu@bnu.edu.cn*
[2] Kitt Peak National Observatory, NOAO, Tucson, AZ 85726-6732, USA
[3] Max-Planck-Institute für Extraterrestrische Physik, D-85740 Garching, Germany

Received 2011 November 11; accepted 2011 December 13

Abstract X-ray loud M dwarfs are a major source of by-products (contamination) in the X-ray band of the multiwavelength quasar survey. As a by-product, the low dispersion spectra of 22 M dwarfs are obtained in which the spectra of 16 sources are taken for the first time. The spectral types and distances of the sample are given based on spectral indices CaH2, CaH3, and TiO5. The parameter $\zeta_{\rm TiO/CaH}$ is calculated to separate the different metallicity classes among dwarfs, subdwarfs and extreme subdwarfs. We also discuss the distributions in the diagrams of $\log(L_{\rm x}/L_{\rm bol})$, the ratio between X-ray and bolometric luminosity versus spectral type and infrared colors.

Key words: spectroscopic — stars: X-rays: M dwarfs

1 INTRODUCTION

Observations from X-ray satellites have shown that strong X-ray emission is a quasi-defining characteristic of Active Galactic Nuclei (AGNs), and X-ray selection from a deep X-ray survey might be the best census method to obtain a sample of AGNs with a high level of completeness (He et al. 2001). The multiwavelength quasar survey (MWQS) aimed at obtaining a sample of $\sim$350 new AGNs brighter than B = 19.0, based on a set of simple yet effective X-ray, radio and optical selection criteria (He et al. 2001; Chen et al. 2002, 2007; Bai et al. 2007). In an X-ray band survey, AGN candidates are selected from the *ROSAT* All-Sky Survey (RASS) sources by applying the criteria to exclude most stars and galaxy clusters (Chen et al. 2007). However, M dwarfs are hard to be distinguished from AGN candidates if criteria in the soft X-ray band alone are applied, thus constituting a potential contaminant to the AGN candidates in optical observations. By analyzing low dispersion spectral characteristics of AGNs and M dwarfs, these two kinds of sources can be differentiated. Thus, the selected X-ray loud M dwarfs can be investigated in detail.

M dwarf stars are the most numerous stars in our galactic neighborhood with masses between 0.1 and 0.5 $M_{\odot}$, and they can be divided into two classes (dM and dMe) based on an optical criterion: dMe stars have Hα in emission, while dM stars have Hα in absorption. Due to the large quantity, longevity (with lifetime greater than the Hubble time), and spectral energy distribution

* Supported by the National Natural Science Foundation of China.

(SED) sensitivity to metallicity (Lépine et al. 2007), M dwarfs are suitable as tracers of the chemical and dynamical evolution of the Galaxy (Laughlin et al. 1997). The optical and near infrared spectra of M dwarfs are dominated by molecular absorption bands of metal oxides and hydrides (Bessell 1991) and the ratio between their strengths has been known as a metallicity diagnostic (Bessell 1982). Four spectroscopic indices (TiO5, CaH1, CaH2, CaH3) were defined by Reid et al. (1995) to separate three metallicity subclasses: M dwarfs (dM), subdwarfs (sdM) and extreme subdwarfs (esdM) (Gizis 1997). Furthermore, the higher radial velocity and deeper transit/occultation that are consequences of the low stellar mass and small radius of M dwarf stars will facilitate the detection of small planets. M dwarfs might be suitable for hosting planets, as indicated by the commonly observed accretion disks around young dwarf stars (Liu et al. 2004; Lada et al. 2006).

In this paper, the initial result of a sample of 22 M dwarfs limited by X-ray flux is given in Section 2. In Section 3, the classification system for M dwarfs and subdwarfs is re-examined based on a combination of four relationships defined in [CaH1, TiO5], [CaH2, TiO5], and [CaH3, TiO5]. The metallicity index $\zeta_{\rm TiO/CaH}$ is calculated to measure the metal content in M dwarfs. A summary is given in Section 4.

2 OBSERVATION AND RESULT

The candidates are selected with criteria in the X-ray band and observed by using the 2.1 m and 2.16 m telescopes at Kitt Peak National Observatory and National Astronomical Observatories, Chinese Academy of Sciences (He et al. 2001; Chen et al. 2002, 2007; Bai et al. 2007; Sun et al. 2011), respectively. The criteria adopted for the selection of candidates are consistent between the two telescopes (Bai et al. 2007). The spectral coverages are respectively about 4000–10 000 Å with resolution of 7 Å and 4000–8000 Å with resolution of 13 Å. All the spectra are reduced with IRAF. The initial result is a subset of 22 M dwarfs, in which the spectra of 16 sources are taken for the first time. A cross identification has been made with the Two Micron All Sky Survey (2MASS) All-Sky Catalog of Point Sources to obtain data in the near infrared band. All of the 2MASS sources lie within $7''$ from the optical position of our targets.

Table 1 displays the ROSAT and 2MASS source designation and optical position. Among 22 M dwarfs, four spectra have Hα in absorption and are classified as dM stars (1RXS J015515.4–173916, 1RXS J041615.7+012640, 1RXS J043426.2–030041, 1RXS J075107.8+061714). Others are classified as dMe stars due to the Hα in emission. Figure 1 shows the spectra of the M dwarfs.

3 DISCUSSION

3.1 Molecular Band Indices

The classification of M dwarfs is based on the strength of the TiO and CaH molecular bands near 7000 Å and three spectral indices, CaH2, CaH3, and TiO5, are defined to measure the mean flux level of the molecular bands (Reid et al. 1995).

In order to obtain the precise spectral indices, we test wavelengths of Hα and find that the wavelengths of the spectra can shift by up to 30 Å because of the long integration times of the M dwarf from 1200 to 3600 seconds. The gravity effect and the change of temperature gradient may cause a displacement between the CCD and spectrograph over such a long integration time. For each spectrum, the central wavelength of Hα is measured carefully to calculate the shift of the molecular band. The molecular band indices are displayed in Table 2. There are discrepancies of molecular band indices between our samples and the six M dwarfs in Riaz et al. (2006), which may be caused by the difference of the spectral resolution. M dwarfs are by-products of the MWQS and low resolution spectra (7–13 Å) are good enough to make AGN identifications.

The distribution of three spectral indices is shown in Figure 2. The TiO and CaH band strengths are tightly correlated in the left frame, which indicates that the stars have equivalent (solar) metallic-

Table 1 Position of M dwarfs

ROSAT Name	2MASS Name	R.A. (2000)	DEC (2000)
1RXS J015515.4–173916	01551663–1739080	01 55 16.32	−17 39 06.9
1RXS J040840.7–270534	04084031–2705473*	04 08 40.24	−27 05 46.0
1RXS J041132.8+023559	04113190+0236058	04 11 31.68	+02 36 05.2
1RXS J041132.8+023559	04113149+0236012	04 11 31.50	+02 36 01.3
1RXS J041325.8–013919	04132663–0139211*	04 13 26.19	−01 39 20.7
1RXS J041612.7–012006	04161320–0119554	04 16 13.12	−01 19 54.1
1RXS J041615.7+012640	04161502+0126570	04 16 14.99	+01 26 57.8
1RXS J042854.3+024836	04285400+0248060	04 28 53.92	+02 48 08.0
1RXS J043051.6–011253	04305207–0112471	04 30 51.71	−01 12 48.7
1RXS J043426.2–030041	04342887–0300390	04 34 28.84	−03 00 39.3
1RXS J053954.8–130805	05395494–1307598*	05 39 54.90	−13 07 59.1
1RXS J055533.1–082915	05553254–0829243*	05 55 32.57	−08 29 25.1
1RXS J060121.5–193749	06012092–1937421	06 01 20.90	−19 37 42.1
1RXS J075107.8+061714	07510760+0617135	07 51 07.63	+06 17 13.3
1RXS J111819.9+134739	11182030+1347392	11 18 20.02	+13 47 41.7
1RXS J112144.4+162156	11213897+1617528	11 21 39.24	+16 17 52.4
1RXS J125336.5+224742	12533626+2247354*	12 53 36.18	+22 47 35.3
1RXS J130123.5+265145	13012236+2651422	13 01 22.09	+26 51 46.4
1RXS J170849.1–110433	17084975–1104308	17 08 50.01	−11 04 25.9
1RXS J174741.0–135445	17474148–1354368	17 47 41.54	−13 54 35.5
1RXS J185008.6+110509	18500888+1105098	18 50 08.64	+11 05 10.4
1RXS J210326.6+161658	21032686+1616569*	21 03 26.80	+16 16 57.6

Notes: $*$ These six sources are contained in the catalog of Riaz et al. (2006).

Table 2 Quantities of M Dwarf Stars

ROSAT Name	cts[a]	HR1[b]	J	H	K	CaH2	CaH3	TiO5	$\zeta_{\rm TiO/CaH}$	SpT[c]	Dist.[d]	$\log \frac{L_{\rm x}}{L_{\rm bol}}$
1RXS J015515.4−173916	0.0622	−0.23	12.268	11.645	11.397	0.72	0.91	0.80	1.19	M0	242	−2.26
1RXS J040840.7−270534	0.0610	−0.08	10.813	10.234	9.975	0.42	0.69	0.43	0.98	M3.5	64	−2.73
1RXS J041132.8+023559	0.0825	0.06	10.416	9.793	9.530	0.58	0.78	0.62	1.01	M1.5	76	−2.77
1RXS J041132.8+023559	0.0825	0.06	10.046	9.428	9.136	0.52	0.78	0.60	0.94	M2	61	−2.93
1RXS J041325.8−013919	0.0976	0.01	9.375	8.761	8.504	0.43	0.69	0.53	0.83	M2.5	40	−3.11
1RXS J041612.7−012006	0.0358	−0.26	12.004	11.429	11.045	0.45	0.74	0.48	1.01	M3	122	−2.60
1RXS J041615.7+012640	0.0211		13.602	12.962	12.768	0.67	0.83	0.74	0.99	M0.5	403	
1RXS J042854.3+024836	0.0203	−1.00	10.809	10.203	9.980	0.56	0.78	0.57	1.08	M2	83	−3.65
1RXS J043051.6−011253	0.0172	0.21	11.403	10.830	10.527	0.39	0.67	0.41	0.96	M4	81	−2.98
1RXS J043426.2−030041	0.0325	0.15	13.141	12.445	12.287	0.78	0.90	0.85	1.08	K7	391	−2.09
1RXS J053954.8−130805	0.0505	−0.24	10.601	9.984	9.724	0.54	0.79	0.60	0.98	M2	80	−2.99
1RXS J055533.1−082915	0.0717	−0.20	10.735	10.168	9.884	0.43	0.68	0.48	0.90	M3	68	−2.74
1RXS J060121.5−193749	0.0956	−0.01	14.104	13.782	13.800	0.45	0.73	0.50	0.96	M3	333	−0.97
1RXS J075107.8+061714	0.0696	0.11	11.866	11.257	10.962	0.68	0.86	0.74	1.08	M0	182	−2.28
1RXS J111819.9+134739	0.1086	−0.47	9.087	8.516	8.258	0.48	0.73	0.55	0.90	M2.5	36	−3.32
1RXS J112144.4+162156	0.0278	−0.39	12.079	11.450	11.195	0.71	0.86	0.73	1.26	M0.5	196	−2.63
1RXS J125336.5+224742	0.0758	−0.12	10.482	9.870	9.634	0.45	0.68	0.48	0.93	M3	60	−2.79
1RXS J130123.5+265145	0.0136	0.30	11.333	10.740	10.512	0.41	0.66	0.48	0.85	M3	90	−3.07
1RXS J170849.1−110433	0.0769	−0.25	10.541	9.953	9.658	0.48	0.72	0.58	0.84	M2	74	−2.84
1RXS J174741.0−135445	0.0552	1.00	11.058	10.395	10.151	0.59	0.80	0.61	1.09	M1.5	100	−2.50
1RXS J185008.6+110509	0.0556	0.43	10.429	9.817	9.541	0.55	0.78	0.58	1.03	M2	71	−2.84
1RXS J210326.6+161658	0.0750	−0.02	11.078	10.430	10.178	0.48	0.73	0.49	1.00	M3	82	−2.55

a: The *ROSAT* count rate is in counts s^{-1}. b: The *ROSAT* hardness ratio, except for one star with an unreliable hardness ratio. c: Spectral type. d: Distance in parsec.

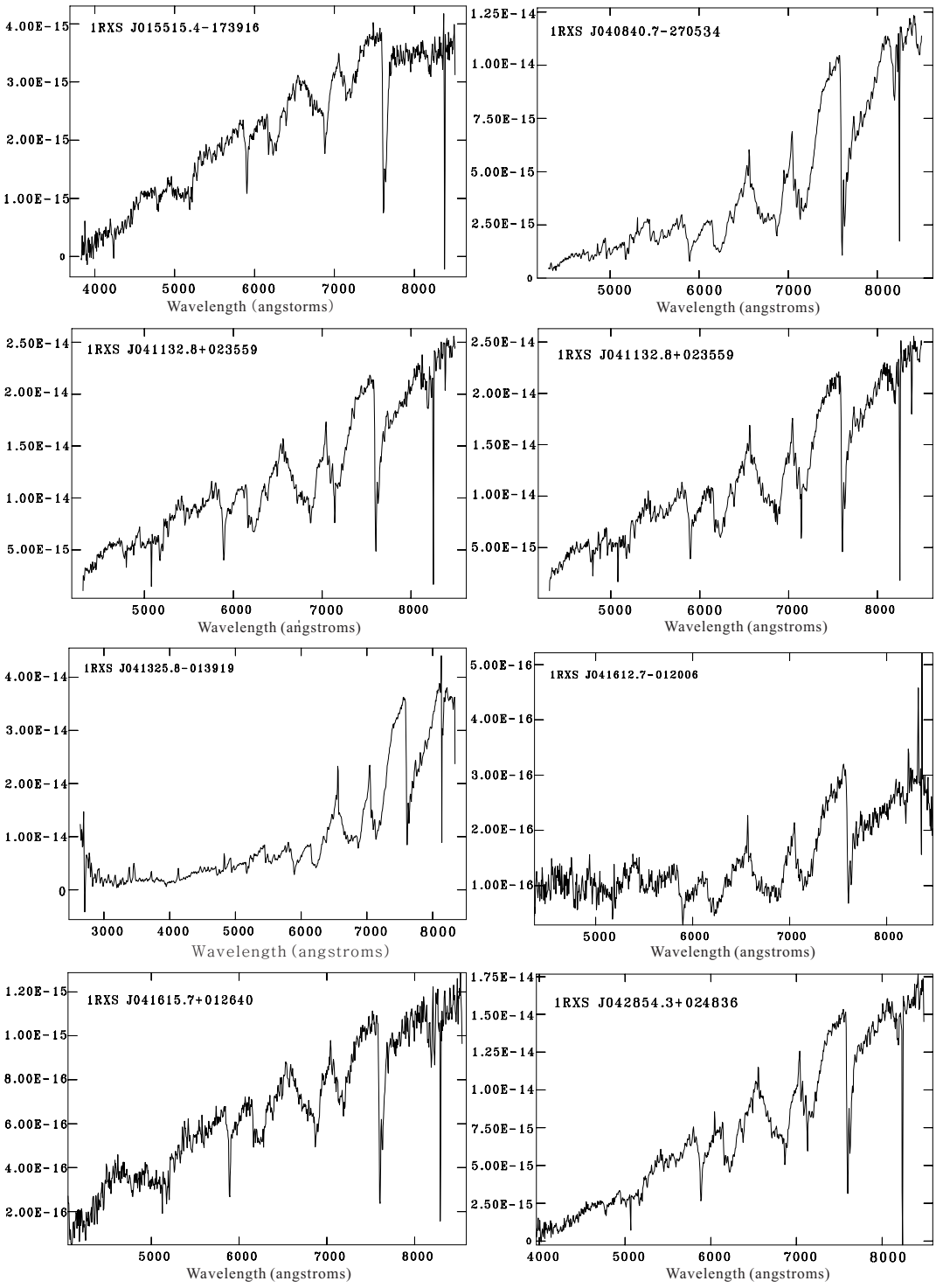

Fig. 1 Spectra of M dwarf stars. Spectral flux (F_λ) is in erg cm^{-2} s^{-1} Å^{-1}.

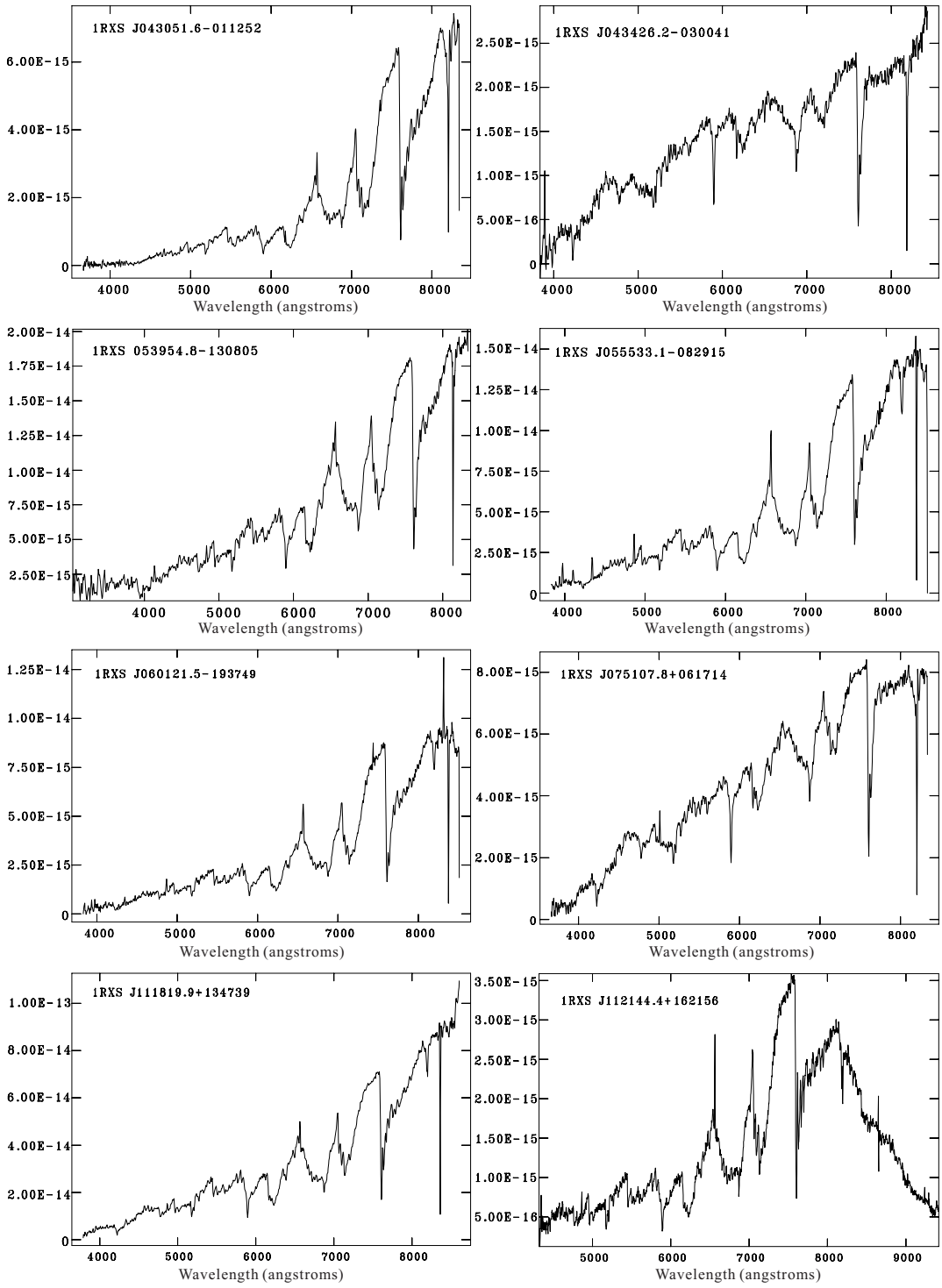

Fig. 1 — *Continued.*

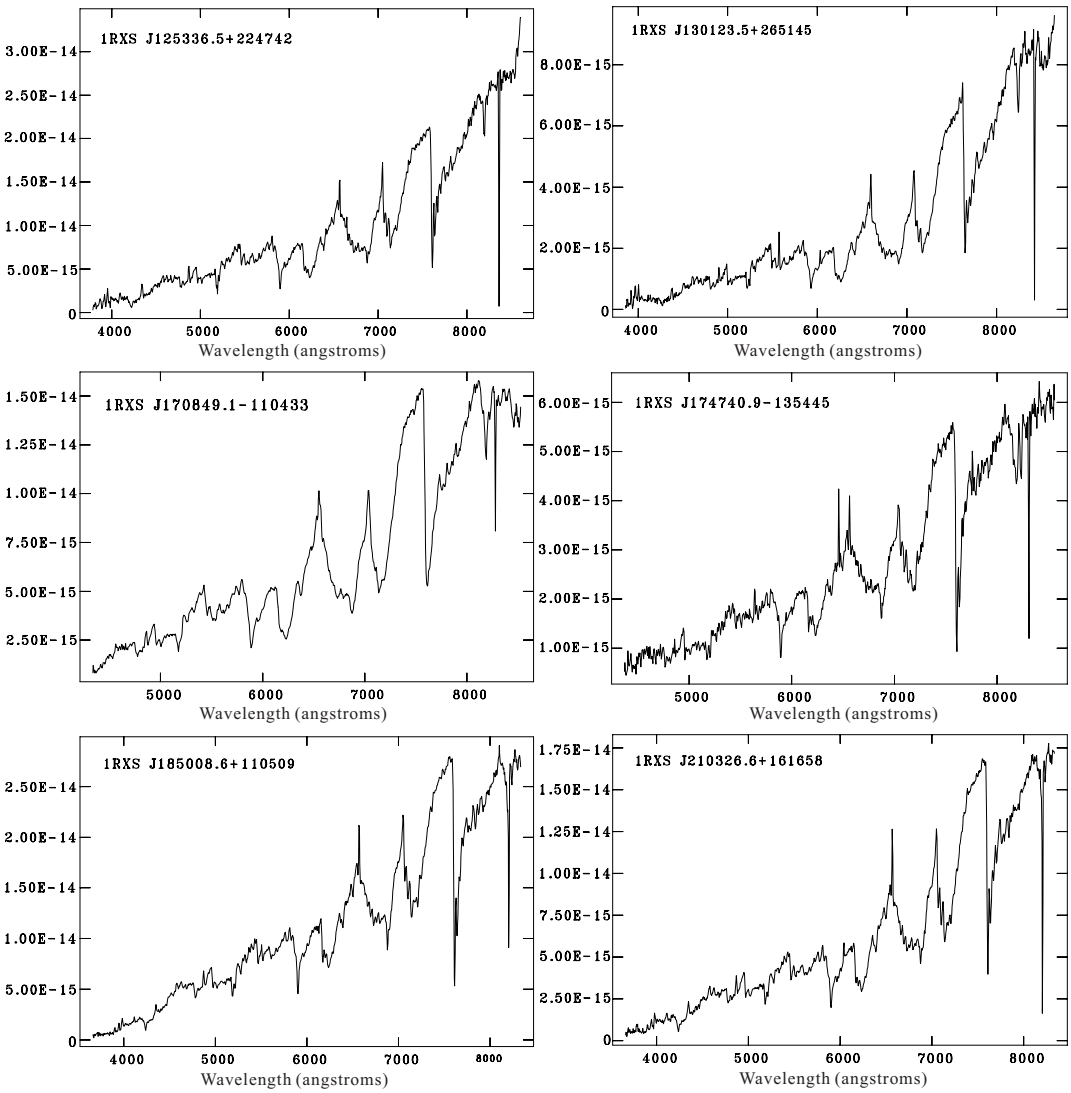

Fig. 1 — *Continued.*

ities and probably belong to Population I (Lépine et al. 2007). The metallicity class separator (*solid line*), proposed by Burgasser & Kirkpatrick (2006), shows that all our stars belong to M dwarfs. The right frame in Figure 2 represents the relation between CaH2 and CaH3. The *dashed line* stands for the fitting of our sample with the least squares method (Eq. (1)). The distribution suggests that CaH2 may be dependent on metallicity (Lépine et al. 2007).

$$\mathrm{CaH3} = -0.516\mathrm{CaH2}^2 + 1.244\mathrm{CaH2} + 0.251\,. \tag{1}$$

We obtain the parameter $\zeta_{\mathrm{TiO/CaH}}$ introduced by Lépine et al. (2007) to make the metallicity class separation among dwarfs, subdwarfs and extreme subdwarfs, based on the relative strength of TiO to CaH. The parameter $\zeta_{\mathrm{TiO/CaH}}$ is defined as

$$\zeta_{\mathrm{TiO/CaH}} = \frac{1 - \mathrm{TiO5}}{1 - [\mathrm{TiO5}]_{\mathrm{Z}_\odot}}\,, \tag{2}$$

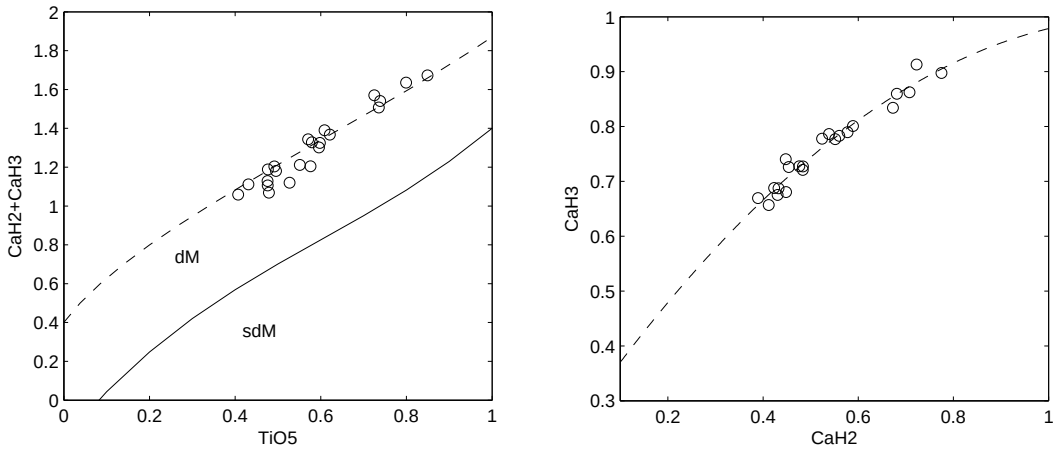

Fig. 2 *Left*: CaH and TiO band strengths of the stars of our sample. The *dashed line* shows the (CaH2+CaH3)/TiO5 relationship of disk M dwarfs in Lépine et al. (2007). The *solid line* shows the metallicity separator. *Right*: Distribution of the CaH2 and CaH3 spectral indices of our sample. The *dashed line* represents the best fitted relationship.

where $[\mathrm{TiO5}]_{Z_\odot}$ is given by Lépine et al. (2007), as a function of the CaH2+CaH3 index. The parameters of our sample are larger than 0.83, which confirms that they belong to M dwarfs with near-solar metallicity.

We have used the relation from Reid et al. (1995) (Eq. (3)) to obtain a spectral type with an uncertainty of ± 0.5 subclasses. The spectral type of our sample ranges between K7 and M4.

$$S_p = -10.775 \times \mathrm{TiO5} + 8.2\,. \tag{3}$$

3.2 Absolute Magnitudes

Riaz et al. (2006) have given an experiential relation (Eq. (4)) between M_J (absolute magnitude in J band) and TiO5 for 35 M dwarfs with TiO5$\geq$0.4, and an rms scatter of 0.8 mag. We used the relation to obtain M_J, and derived the bolometric magnitudes from the absolute K magnitudes (Veeder 1974). The distance to our stars was estimated by the absolute magnitudes with uncertainties on the order of $\pm 37\%$. There are 14 stars, over half of the sample, which lie within 100 pc. It has to be pointed out that stars that lie in the region around TiO5$\sim$4 have a high uncertainty in their absolute magnitude and their derived distance (Riaz et al. 2006).

$$M_J = 0.97(\mathrm{TiO5})^2 - 5.01(\mathrm{TiO5}) + 8.73\,. \tag{4}$$

3.3 Luminosity

We have used the relation of the count rate to energy flux conversion (Schmitt et al. 1995) to obtain X-ray fluxes for our targets, except for one star with an unreliable hardness ratio. The X-ray luminosity was calculated with the X-ray flux and distance. The strong X-ray luminosity has 20 targets with L_x larger than 10^{29}, and one with L_x larger than $10^{28.5}$, suggesting that they have strong coronal activity (Barrado y Navascués et al. 1998).

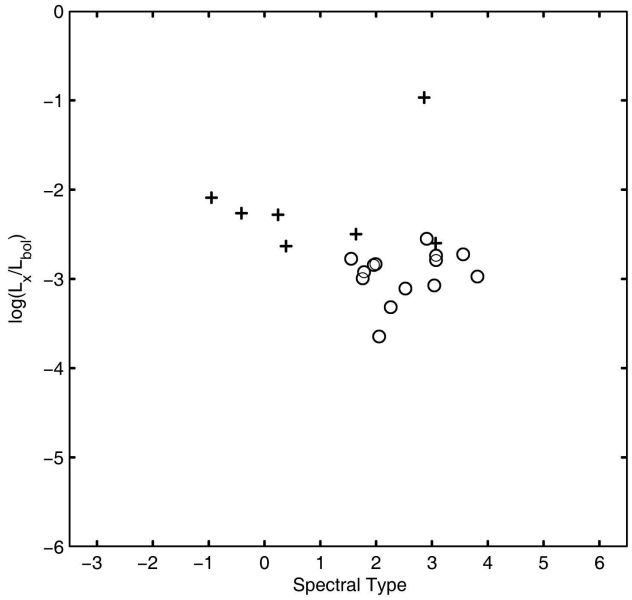

Fig. 3 $\log(L_{\rm x}/L_{\rm bol})$ versus spectral type. *Pluses* are targets with distance larger than 100pc and *circles* represent targets with distance less than 100pc.

The distribution between $\log(L_{\rm x}/L_{\rm bol})$ and the spectral type is shown in Figure 3. For a given spectral type, there is a large spread in $L_{\rm x}$, as shown in fig. 5 of Riaz et al. (2006). The differences in rotational velocity can explain this dispersion in $L_{\rm x}$ for low-mass stars (Stauffer et al. 1997). The distribution also suggests that samples with different distances are located in different areas of the diagram. Our samples with distances exceeding 100pc are inclined to be stronger X-ray emitters and earlier type stars than ones within 100pc, but we need more samples to confirm the trend. The distribution of X-ray flux for dM and dMe stars is also tested but no break is found.

3.4 Infrared Colors

M dwarfs cannot be directly distinguished from AGN samples if criteria in the soft X-ray band alone are applied, but with colors in the infrared band there may be hints to differentiate the two kinds of sources.

Figure 4 shows the color-color diagram in the infrared band for M dwarfs and AGN samples (Chen et al. 2007). Colors of AGNs are distributed widely in the diagram because of the complex hot dusty environment outside the accretion disks with a distance of a few parsecs to the central black holes. However, M dwarfs are concentrated in a smaller area of the color-color diagram, and this may indicate that the temperatures of their atmosphere cover a narrow range from $\sim$2100 K to $\sim$3300 K.

Chen et al. (2007) suggested that most AGNs span a color range of $1.0 < J - K < 2.0$ and $0.5 < H - K < 1.2$, while Riaz et al. (2006) selected M dwarfs with criteria $0.8 < J - K < 1.1$, $H - K > 0.15$ and $J - H < 0.75$. Most of our targets agree with the criteria of Riaz et al. (2006), but one M dwarf lies outside the range. Color indices for our sample are in ranges of about

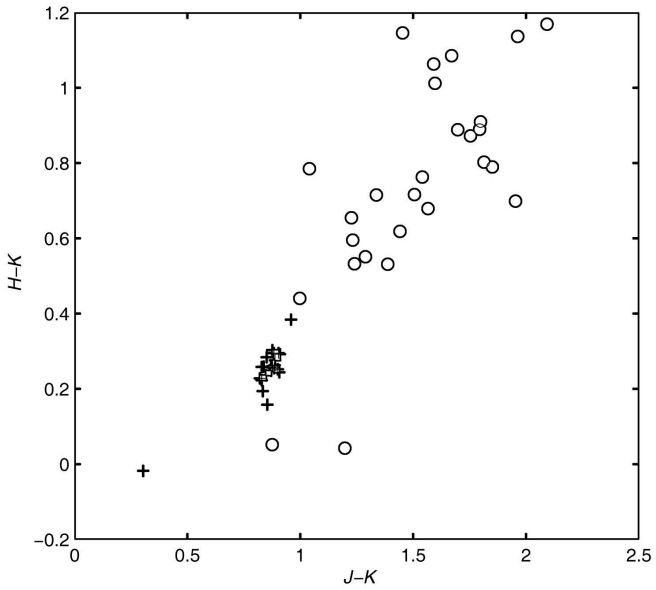

Fig. 4 Infrared color diagram for M dwarfs and AGNs. *Pluses* denote M dwarfs. *Circles* denote the AGN sample in Chen et al. (2007).

$0.76 < J - K < 0.96$, $H - K > 0.14$, and $J - H < 0.56$. The infrared colors may be effective for distinguishing M dwarfs from AGNs.

4 SUMMARY

As a by-product in the MWQS, we have obtained the spectra of 22 X-ray flux limited M dwarf stars. The spectral types are calculated with molecular band indices based on a calibration of the TiO to CaH band strength ratio, ranging from K7 to M4. Over half of them lie within 100pc of the Sun. The distribution between $\log(L_{\rm x}/L_{\rm bol})$ and the spectral type suggests that M dwarfs with different distances may be located in different areas of the diagram and the large spread in X-ray luminosities for a given spectral type reflects the range of rotational velocities of the stars. The infrared colors could be criteria to separate AGNs from M dwarfs selected from soft X-ray data. For future observations, we are going to enlarge the samples up to 100 and a further investigation on the X-ray luminosity function may provide more information about coronal heating mechanisms and occurrence of flares. An observational campaign is on the schedule, aimed at obtaining a frequency spectrum of dM and dMe stars based on photometric observations to characterize M dwarf variations, which will give us a chance to study the interior pulsation models of M dwarfs. Extrasolar planet candidates may be selected if we can acquire long term photometric observations and high resolution spectral observations.

Acknowledgements This work was supported by the Scientific Research Foundation of Beijing Normal University and the National Natural Science Foundation of China (Grant No. 10778717). This work was partially supported by the Open Project Program of the Key Laboratory of Optical Astronomy, National Astronomical Observatories, Chinese Academy of Sciences.

References

Bai, Y., Chen, Y., He, X.-T., et al. 2007, ChJAA (Chin. J. Astron. Astrophys.), 7, 375
Barrado, D., Stauffer, J. R., & Randich, S. 1998, ApJ, 506, 347
Bessell, M. S. 1982, Proceedings of the Astronomical Society of Australia, 4, 417
Bessell, M. S. 1991, AJ, 101, 662
Burgasser, A. J., & Kirkpatrick, J. D. 2006, ApJ, 645, 1485
Chen, Y., Bai, Y., He, X.-T., et al. 2007, ChJAA (Chin. J. Astron. Astrophys.), 7, 595
Chen, Y., He, X.-T., Wu, J.-H., et al. 2002, AJ, 123, 578
Gizis, J. E. 1997, AJ, 113, 806
He, X.-T., Wu, J.-H., Yuan, Q.-R., et al. 2001, AJ, 121, 1863
Lada, C. J., Muench, A. A., Luhman, K. L., et al. 2006, AJ, 131, 1574
Laughlin, G., Bodenheimer, P., & Adams, F. C. 1997, ApJ, 482, 420
Lépine, S., Rich, R. M., & Shara, M. M. 2007, ApJ, 669, 1235
Liu, M. C., Matthews, B. C., Williams, J. P., & Kalas, P. G. 2004, ApJ, 608, 526
Reid, I. N., Hawley, S. L., & Gizis, J. E. 1995, AJ, 110, 1838
Riaz, B., Gizis, J. E., & Harvin, J. 2006, AJ, 132, 866
Schmitt, J. H. M. M., Fleming, T. A., & Giampapa, M. S. 1995, ApJ, 450, 392
Stauffer, J. R., Balachandran, S. C., Krishnamurthi, A., et al. 1997, ApJ, 475, 604
Sun, Y.-C., Bai Y., He X.-T. et al. 2011, Progress in Astronomy, accepted
Veeder, G. J. 1974, AJ, 79, 1056